POLITECNICO DI TORINO
Repository ISTITUZIONALE

PSO-assisted extraction of VCSEL parameters from L-I and S21 measurements

Original
PSO-assisted extraction of VCSEL parameters from L-I and S21 measurements / Marchisio, Andrea; Carena, Andrea; Curri, Vittorio; Bardella, Paolo. - ELETTRONICO. - (2024), pp. 49-50. (International Conference on Numerical Simulation of Optoelectronic Devices (NUSOD) New Delhi (India) 23-27 September 2024) [10.1109/NUSOD62083.2024.10723706].

Availability:
This version is available at: 11583/2992680 since: 2024-09-23T09:31:08Z

Publisher:
IEEE

Published
DOI:10.1109/NUSOD62083.2024.10723706

Terms of use:

This article is made available under terms and conditions as specified in the corresponding bibliographic description in the repository

Publisher copyright
IEEE postprint/Author's Accepted Manuscript

©2024 IEEE. Personal use of this material is permitted. Permission from IEEE must be obtained for all other uses, in any current or future media, including reprinting/republishing this material for advertising or promotional purposes, creating new collecting works, for resale or lists, or reuse of any copyrighted component of this work in other works.

(Article begins on next page)

08 May 2026

PSO-assisted extraction of VCSEL parameters from L-I and S21 measurements

Andrea Marchisio
DET
Politecnico di Torino
Torino, Italy
andrea_marchisio@polito.it

Andrea Carena
DET
Politecnico di Torino
Torino, Italy
andrea.carena@polito.it

Vittorio Curri
DET
Politecnico di Torino
Torino, Italy
vittorio.curri@polito.it

Paolo Bardella
DET
Politecnico di Torino
Torino, Italy
paolo.bardella@polito.it

***Abstract*—We propose a method based on particle swarm optimization for the extraction of VCSELs rate-equation model parameters from experimental power and S21 measurements. The method is shown to reliably predict a set of parameters for accurate reproduction of the measured curves.**

***Index Terms*—VCSEL, Parameter Extraction, Particle Swarm Optimization**

I. Introduction

Vertical-Cavity Surface-Emitting Lasers (VCSELs) are experiencing an ever-growing success due to multiple inherent features, such as low threshold current, high quantum efficiency, and high-speed modulation at low current[1]. Due to these advantages, VCSELs are becoming popular choices in a wide spectrum of applications, ranging from data communication to optical sensing. However, modeling their behavior is complicated: thermal effects such as thermal rollover, and complex physical effects, such as spatial hole burning, must be taken into account [2] for a reliable description of the device. Then, the extraction of fitting parameters from experimental measurements of a potentially unknown device (for instance, for subsequent numerical circuit-level simulations) is difficult.

For this purpose, instead of using time-consuming brute-force approaches or resource-intensive machine learning (ML) methods, where hundreds of thousands of good-quality samples are required to effectively train the network, an optimization algorithm could be chosen to perform one-off parameter extraction from the experimental reference directly. In this work, we expand the work of [3], by applying a refined PSO algorithm [4] to a set of experimental L-I and S21 response measurements of a a GaAs/AlGaAs $850\,\mathrm{nm}$ VCSEL, characterized by a 1λ-cavity with three $8\,\mathrm{nm}$ GaAs quantum wells [5, 6], thus demonstrating that this approach can perform accurate predictions even when dealing with non-ideal curves.

II. VCSEL model and extraction algorithm

In this work, since we are targeting fast numerical simulations, we employ a rate equation-based model [2], which captures both the evolution over time of carrier populations and photons, and the thermal effects by means of three empirical equations describing the temperature dependencies.

This model introduces the spatial dependency of the carrier and photon numbers by considering a two-term Bessel expansion of the carriers distribution in the radial direction r:

$$N(r,t) = N_0(t) - N_1(t)J_0(\sigma_1 r/R) \tag{1}$$

with σ_1 first nonzero root of J_1, J_0 and J_1 Bessel functions of the first kind, and R effective radius of the active layer. The temporal evolution of the expansion coefficients $N_0(t)$ and $N_1(t)$ is given by the following spatially independent rate equations:

$$\frac{\mathrm{d}N_0}{\mathrm{d}t} = \frac{\eta_\mathrm{i} I}{q} - \frac{N_0}{\tau_\mathrm{n}} - \frac{I_\mathrm{l}(N_0,T)}{q} - -\frac{G(T)\left[\gamma_{00}\tilde{N} - \gamma_{01}N_1\right]}{1+\epsilon S}S \tag{2}$$

$$\frac{\mathrm{d}N_1}{\mathrm{d}t} = -\frac{N_1}{\tau_\mathrm{n}}(1+h_\mathrm{diff}) + \frac{G(T)\left[\phi_{100}\tilde{N} - \phi_{101}N_1\right]}{1+\epsilon S}S \tag{3}$$

with $\tilde{N} = N_0 - N_\mathrm{tr}(T)$, η_i injection efficiency, I bias current, q electron charge, τ_n carrier lifetime, T temperature, $G(T)$ gain coefficient, $N_\mathrm{tr}(T)$ transparency carrier number, $I_\mathrm{l}(N_0,T)$ leakage current, ϵ gain compression factor, h_diff diffusion coefficient. The coefficients γ_{00}, γ_{01}, ϕ_{100}, ϕ_{101} quantify the overlap between the fundamental transverse mode and the active region. The termal effects are introduced by an equation that describes the thermal evolution of the temperature in the device and by a set of empirical equations for gain coefficient, transparency carrier number, and leakage current [3]:

$$T = T_\mathrm{amb} + (IV - P_\mathrm{out})R_\mathrm{th} - \tau_\mathrm{th}\frac{\mathrm{d}T}{\mathrm{d}t} \tag{4}$$

with V applied voltage, T_amb ambient temperature, R_th thermal impedance, and τ_th thermal time constant. Finally,

$$G(T) = G_0'\frac{1 + a_{\mathrm{g}_1}'T + a_{\mathrm{g}_2}'T^2}{1 + b_{\mathrm{g}_1}'T + b_{\mathrm{g}_2}'T^2} \tag{5}$$

$$N_\mathrm{tr}(T) = N_{\mathrm{tr}_0}'\left(1 + C_{\mathrm{n}_1}'T + C_{\mathrm{n}_2}'T^2\right) \tag{6}$$

$$I_\mathrm{l}(N_0,T) = I_{\mathrm{l}_0}\exp\left(\frac{-a_0 + a_1N_0 + a_2N_0T - a_3/N_0}{T}\right) \tag{7}$$

contain fitting parameters that can be independently extracted to describe the thermal behavior.

The goal of this analysis is to extract from the L-I and small signal measurements a set of 20 parameters to accurately reproduce the behavior of the device under test. Table I reports the 20 target parameters, together with their associated ranges for the bounded optimization procedure.

Particle Swarm Optimization (PSO) is a cooperative evolutionary algorithm where a set of N agents, called "particles",

TABLE I: Investigated VCSEL parameters and their ranges for the bounded extraction.

Parameters	Range	Parameters	Range
Injection efficiency η_i	0.70 to 1.00	Transp. num. N'_{tr_0}	2.00×10^6 to 1.00×10^8
Power coeff. k_f (nW)	10.00 to 60.00	Transp. num. coeff. C'_{n_1} (kK^{-1})	-100.00 to -1.00
Carrier lifetime τ_n (ns)	0.50 to 5.00	Transp. num. coeff. C'_{n_2} (kK^{-2})	0.00 to 100.00
Photon lifetime τ_p (ps)	1.50 to 3.50	Leakage current factor I_{l_0} (A)	1.00 to 2.00
Gain coeff. G'_0 (ms^{-1})	-360.0 to -11.1	Leakage current coeff. a_0 (K)	2.00×10^3 to 1.00×10^4
Gain coeff. a'_{g_1} (kK^{-1})	-5.00 to -0.50	Leakage current coeff. a_1 (K)	0.00 to 3.00×10^{-4}
Gain coeff. a'_{g_2} (kK^{-2})	-50.00 to -2.00	Leakage current coeff. a_2	1.00×10^{-9} to 4.00×10^{-8}
Gain coeff. b'_{g_1} (kK^{-1})	-100 to 0	Diffusion parameter h_diff	1.00 to 20.00
Gain coeff. b'_{g_2} (kK^{-2})	5.56 to 900.0	Thermal impedance R_th (K/W)	5.00×10^2 to 8.00×10^3
Gain saturation factor ϵ	1×10^{-6} to 3×10^{-6}	Spont. emission coeff. β_sp	1×10^{-5} to 9×10^{-6}

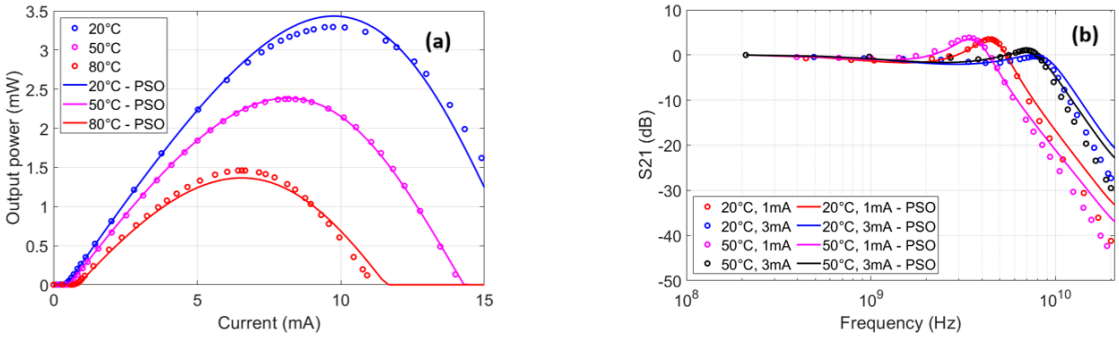

Fig. 1: PSO predictions (solid lines) compared with measurements (circles) for L-I curves [5] (a) and S21 responses [6] (b).

move in a M-dimensional solution space [7], where $M = 20$ is the number of variables to optimize. The movement of the particles depends both on a personal tendency to explore the space and on a social pull towards the best position encountered by the population. This is implemented with two simple equations, that describe the velocity and position of the j-th particle at iteration $k+1$:

$$\mathbf{v}_j^{k+1} = c_\mathrm{i}\mathbf{v}_j^k + c_\mathrm{c}r_1(\mathbf{p}_j^k - \mathbf{x}_j^k) + c_\mathrm{s}r_2(\mathbf{p}_\mathrm{gl}^k - \mathbf{x}_j^k) \quad (8)$$

$$\mathbf{x}_j^{k+1} = \mathbf{x}_j^k + \mathbf{v}_j^{k+1} \quad (9)$$

with c_i inertia coefficient, c_c cognitive acceleration coefficient, c_s social acceleration coefficient, r_1 and r_2 random scaling factors, $\mathbf{p}_j^k$ personal best position for the j-th particle, and $\mathbf{p}_\mathrm{gl}^k$ global best position. Like any other stochastic optimization algorithms, PSO suffers from the exploitation-exploration trade-off: if the particles focus too much on exploration (high c_c), we will never reach convergence; if the the particles focus too much on exploitation (high c_s), we will have premature convergence to a local minimum, which does not represent our target solution. Many different solutions have been proposed to mitigate this effect. One of them is a variation of the PSO called Adaptive PSO [4], which consists of dynamically adapting the acceleration coefficients during the optimization.

The optimization target are three experimental L-I curves [5] at $T = 20\,^\circ\mathrm{C}$, $50\,^\circ\mathrm{C}$, and $80\,^\circ\mathrm{C}$, and four experimental S21 responses [6] measured at four different combinations of temperatures and currents (I=1 mA and 3 mA, for T=20 °C and 50 °C). The algorithm tries to minimize the loss computed as the average of the errors between the reference curves and the predicted ones, computed as $||y_\mathrm{ref} - y_\mathrm{pred}||/||y_\mathrm{ref}||$.

III. Results and Discussion

Fig. 1 reports the reference curves [5, 6] and the curves generated with the predicted parameters for the L-I curves (a) and the S21 responses (b). We successfully captured the threshold, slope, and thermal roll-off of the L-I curves, as well as the peak frequency and the -3 dB bandwidth of the S21 responses. The minor discrepancies with the data can be attributed to measurement noise and the simplicity of the rate-equation based model that we used. Although this model cannot capture higher-order effects, it is essential for demonstrating the validity of the PSO-based approach and for system-level simulations in general.

IV. Acknowledgments

The Authors thank Dr. P. Debernardi, Dr. V. Torrelli and Dr. A. Gullino for proving the measured VCSEL data.

References

[1] A. Liu et al. “Vertical-cavity surface-emitting lasers for data communication and sensing”. In: *Photonics Res.* 7.2 (2019).

[2] P. Mena et al. “A comprehensive circuit-level model of vertical-cavity surface-emitting lasers”. In: *J. Light. Technol.* 17.12 (1999).

[3] A. Marchisio et al. “Particle swarm optimization-assisted approach for the extraction of VCSEL model parameters”. In: *Opt. Lett.* 49.1 (2024).

[4] Z.-H. Zhan et al. “Adaptive particle swarm optimization”. In: *IEEE Trans. Syst. Man. Cybern. B Cybern.* 39.6 (2009).

[5] P. Debernardi et al. “Probing thermal effects in VCSELs by experiment-driven multiphysics modeling”. In: *IEEE J. Sel. Top. Quantum Electron.* 25.6 (2019).

[6] A. Gullino et al. “Modulation response of VCSELs: a physics-based simulation approach”. In: *Proceedings of NUSOD 2020*. 2020.

[7] J. Kennedy et al. “Particle swarm optimization”. In: *Proceedings of ICNN ’95*. Vol. 4. 1995.